35. G. W. Brudvig and R. H. Crabtree, *Proc. Natl. Acad. Sci. U.S.A.* **83**, 4586 (1986).
36. G. Christou and J. B. Vincent, *Biochim. Biophys. Acta* **895**, 259 (1987).
37. O. Burghaus, V. J. DeRose, W. Liang, V. K. Yachandra, M. P. Klein, in *Research in Photosynthesis*, N. Murata, Ed. (Kluwer, Dordrecht, Netherlands, 1992), vol. II, pp. 109–113.
38. Here, EPR silent refers to a conventional EPR experiment in which one detects transitions in a half-integral spin system. However, we have detected paramagnetism in the S_1 state by using parallel-polarization–mode EPR, a method used for observing EPR transitions from integer or non-Kramers spin systems. S. L. Dexheimer and M. P. Klein, *J. Am. Chem. Soc.* **114**, 2821 (1992).
39. A. Haddy, W. R. Dunham, R. H. Sands, R. Aasa, *Biochim. Biophys. Acta* **1099**, 25 (1992).
40. We propose that the coupling within the Mn_2(III,IV) and Mn_2(IV,IV) units is antiferromagnetic. Ferromagnetic coupling of the S = 1/2 ground state of the Mn_2(III,IV) cluster with a S = 2 excited state of the Mn_2(IV,IV) cluster results in the formation of the S = 5/2 ground state. Antiferromagnetic coupling of the S = 1/2 ground state of the Mn_2(III,IV) cluster with the S = 0 state of the Mn_2(IV,IV) cluster results in an S = 1/2 state.
41. V. J. DeRose *et al.*, *Biochemistry* **30**, 1335 (1991).
42. J. J. Riggs, R. Mei, C. F. Yocum, J. E. Penner-Hahn, *J. Am. Chem. Soc.* **114**, 10650 (1992).
43. We thank W. Armstrong, G. Christou, T. Collins, J.-J. Girerd, D. Hodgson, and K. Wieghardt for providing all of the Mn model complexes. We thank H. Dau, T. Roelofs, W. Liang, and J. Andrews for discussions about this work. We are grateful to D. B. Goodin, A. E. McDermott, R. D. Guiles, J. L. Cole, R. D. Britt, J.-L. Zimmermann, S. L. Dexheimer, and D. Kim for their contributions, and to M. Grush for help with XAS data collection. This work was supported by National Science Foundation grant DMB91-04104 and by the director, Division of Energy Biosciences, Office of Basic Energy Sciences, Department of Energy (DOE), under contract DE-AC03-76SF00098. M.P.K. thanks the A. von Humboldt Foundation for a Senior U.S. Scientist Award. Synchrotron radiation facilities were provided by the Stanford Synchrotron Radiation Laboratory (SSRL) and the National Synchrotron Light Source (NSLS), both supported by DOE. The Biotechnology Laboratory at SSRL and Beam Line X9-A at NSLS are supported by the National Center for Research Resources of the National Institutes of Health.

23 November 1992; accepted 1 March 1993

Reversal of Left-Right Asymmetry: A Situs Inversus Mutation

Takahiko Yokoyama, Neal G. Copeland, Nancy A. Jenkins, Charles A. Montgomery, Frederick F. B. Elder, Paul A. Overbeek*

A recessive mutation was identified in a family of transgenic mice that resulted in a reversal of left-right polarity (situs inversus) in 100 percent of the homozygous transgenic mice tested. Sequences that flanked the transgenic integration site were cloned and mapped to mouse chromosome 4, between the *Tsha* and *Hxb* loci. During early embryonic development, the direction of postimplantation turning, one of the earliest manifestations of left-right asymmetry, was reversed in homozygous transgenic embryos. This insertional mutation identifies a gene that controls embryonic turning and visceral left-right polarity.

The establishment of embryonic axes is essential for vertebrate development, but the molecular factors that define vertebrate embryonic polarity remain unknown. Left-right asymmetries are the last to appear in embryonic development and are reflected in the position and structure of the visceral organs such as the heart, stomach, spleen, and liver. Mutations that result in a mirror-image reversal of left-right visceral asymmetry have been described in mice (the inversus viscerum or *iv* mutation) (*1*, *2*) and in humans (*3*, *4*), but these mutants reverse left-right polarity only approximately 50% of the time. This suggests that these mutations produce an indeterminate condition of laterality (*5*) or random determination of polarity (*2*). Here, we report a recessive insertional mutation that results in situs inversus in 100% of homozygous transgenic mice.

The transgenic family OVE210 was generated by microinjection of the Ty811C tyrosinase minigene into one-cell–stage embryos of the inbred albino mouse strain FVB/N (*6*). At birth, transgenic mice can be identified by the presence of pigmentation in their eyes; hemizygous adult mice have light brown fur pigmentation. Southern (DNA) hybridizations to tail DNAs revealed that the OVE210 mice have a single site of transgene integration with a low copy number (one to two copies per genome) (*7*). When hemizygous transgenic OVE210 mice were mated together to generate homozygous mice, no viable adult homozygotes were obtained. Inspection of newborn mice revealed that some of the mice had stomachs located on the right side instead of the left side of the abdomen (Fig. 1A). These mutant mice exhibited severe jaundice (*7*), did not increase in size or weight after birth (Fig. 1A), and did not survive beyond 7 days of age. Dissection of the mutant newborns revealed that they had a common pattern of situs inversus; each had its stomach and spleen (Fig. 1B) located on the right side instead of the left side of the abdomen. Orientations of the heart (Fig. 1B), lungs, and liver were also mirror-image left-right inversions.

To determine the percentage of embryos with situs inversus, we mated hemizygote OVE210 mice and terminated the pregnancies between embryonic day 16 (E16) and E19. The fetuses were assayed for ocular pigmentation and visceral orientation. Out of a total of 74 fetuses, 16 (22%) were albino with normal polarity, 41 (55%) were pigmented with normal polarity, and 17 (23%) were pigmented and had situs inversus, which suggests that insertion of the transgene had caused a recessive mutation. Fifteen of the situs inversus mice were examined in detail. All 15 had left-right reversal of their abdominal visceral organs, one had polysplenia, and one had normal cardiovascular orientation (levocardia) even though the abdominal viscera were inverted (a condition termed heterotaxia). Histological examination of the visceral organs revealed that the mutant mice had significant kidney pathology with dilated tubules and abnormal glomeruli (*7*). When assayed by Southern hybridization, the fetus with heterotaxia was found to be homozygous for the transgenic insertion.

Kartagener's syndrome (*3*) is an autosomal recessive disorder in humans characterized by situs inversus. The syndrome is associated with chronic sinusitis and pulmonary disease, in addition to infertility in males. Patients with Kartagener's syndrome exhibit defective dynein arms in their cilia (*8*). To assess whether the transgenic mice with situs inversus might have a similar defect, we collected tracheae from mutant and control mice and examined the tracheal cilia by electron microscopy. No defects in the dynein arms were observed in the transgenic mutants (*9*).

To begin molecular characterization of this new insertional mutation, we constructed a genomic library of OVE210 DNA (*10*–*13*). Four overlapping clones containing the transgenic integration site were obtained (Fig. 2A). One clone (clone 4) contains the entire transgenic insert (two tandem copies of the transgene). A 2.0-kb Hind III fragment (p3.2H) (Fig. 2A) that contained single-copy genomic sequences was used as a probe in Southern hybridizations to verify that the mutant mice were

T. Yokoyama, Department of Cell Biology, Baylor College of Medicine, Houston, TX 77030.
N. G. Copeland and N. A. Jenkins, Mammalian Genetics Laboratory, ABL–Basic Research Program, National Cancer Institute, Frederick Cancer Research and Development Center, Frederick, MD 21702.
C. A. Montgomery, Center for Comparative Medicine, Baylor College of Medicine, Houston, TX 77030.
F. F. B. Elder, Department of Pathology and Laboratory Medicine, University of Texas Health Science Center, Houston, TX 77030.
P. A. Overbeek, Department of Cell Biology, Institute for Molecular Genetics, and Howard Hughes Medical Institute, Baylor College of Medicine, Houston, TX 77030.

*To whom correspondence should be addressed.

homozygous for the transgenic insert. After digestion of genomic DNA with Eco RI, nontransgenic mice had a single hybridization band at 9.2 kb. In contrast, pigmented mice with normal left-right polarity had two bands (one at 9.2 kb and the other near 18 kb), and situs inversus mutants had only the transgenic band at 18 kb (Fig. 2B). Sixty-four mice, including 14 mice with situs inversus, were tested by Southern hybridization with probe p3.2H. All mice with situs inversus were homozygous for the transgenic insert, whereas all mice with normal polarity were hemizygous or nontransgenic. These results support the hypothesis that the transgenic insertion produced a recessive mutation in an endogenous gene that dictates left-right laterality. It is unlikely that expression of the tyrosinase minigene causes the situs inversus phenotype because ten additional independent transgenic families have been generated by microinjection of the Ty811C tyrosinase transgene (6), and none of the hemizygous or homozygous mice in these other families shows situs inversus.

To test for allelism with the previous *iv* mutation, we mated transgenic hemizygotes to mice of the inbred strain SI/Col, which are homozygous for the *iv* mutation (*1*, *2*). Of 28 offspring, 15 were transgenic for Ty811C. All 15 showed normal left-right polarity and normal viability, which indicates that the insertional mutation is not allelic to *iv*. We have named the locus defined by the transgenic insertion "inversion of embryonic turning" (*inv*).

Because the *inv* mutation was not allelic to *iv*, the chromosomal location of probe p3.2H was determined by interspecific backcross analysis with the use of progeny derived from matings of (C57BL/6J × *Mus spretus*)F_1 mice with C57BL/6J mice. This interspecific backcross mapping panel has been typed for over 1100 loci that are well distributed among all of the autosomes as well as the X chromosome (*14*). Two M.

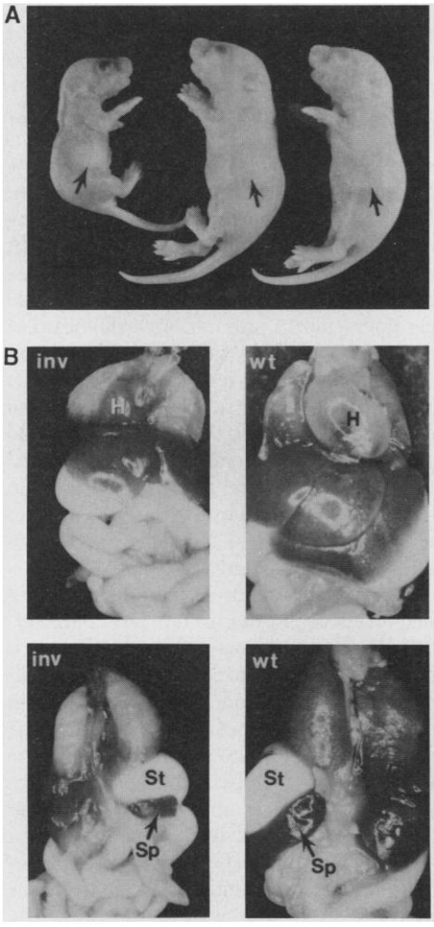

Fig. 1. Situs inversus phenotype. (**A**) Five-day-old mice of transgenic family OVE210. Arrows indicate stomachs. The two transgenic mice (left and center) can be recognized by their ocular pigmentation. The mouse with situs inversus (on the left) failed to grow in comparison to its littermates with normal polarity (center and right). (**B**) Ventral (top row) and dorsal (bottom row) views of mutant (inv) and control (wt) viscera dissected from mice at 3 days of age. H, Sp, and St indicate heart, spleen, and stomach, respectively. The visceral organs are mirror-image inverted (relative to the sagittal midline) in the mutant mice.

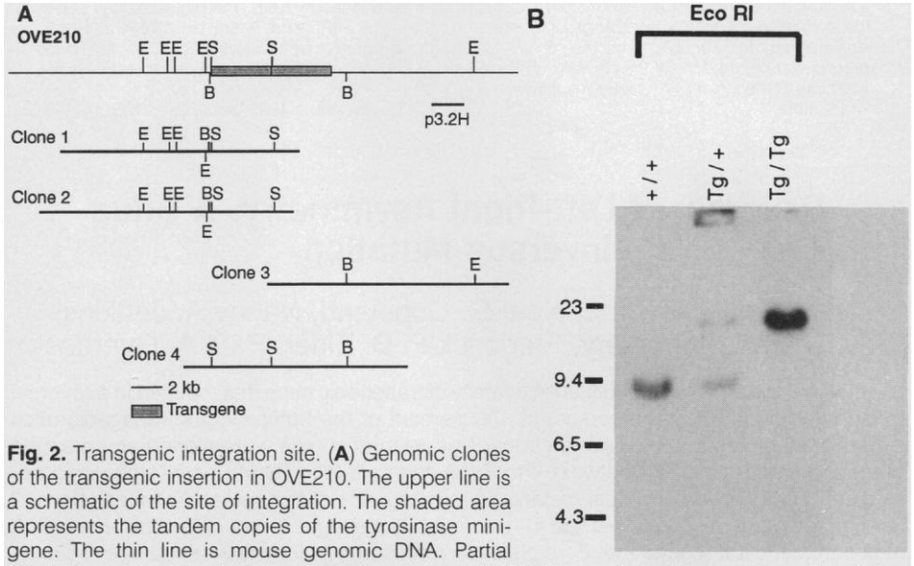

Fig. 2. Transgenic integration site. (**A**) Genomic clones of the transgenic insertion in OVE210. The upper line is a schematic of the site of integration. The shaded area represents the tandem copies of the tyrosinase minigene. The thin line is mouse genomic DNA. Partial restriction maps of the four clones isolated from the OVE210 genomic library are shown. Restriction sites indicated are Eco RI (E), Bam HI (B), and Sal I (S). Probe p3.2H contains single-copy genomic sequences isolated from clone 3. (**B**) Restriction fragment length polymorphism (RFLP) in OVE210 mice. Ten micrograms of genomic DNA from nontransgenic (+/+), transgenic with normal polarity (Tg/+), or transgenic with situs inversus (Tg/Tg) mice was digested with Eco RI and electrophoresed in a 0.8% agarose gel. DNAs were transferred onto a nylon membrane (Zeta-probe; Bio-Rad) then hybridized to the p3.2H fragment that was labeled with [^{32}P]dCTP by the random primer method (*27*). Molecular weight markers (λ DNA digested with Hind III) are indicated on the left.

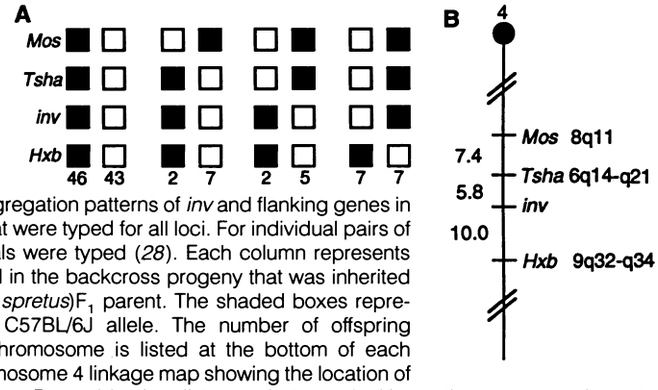

Fig. 3. Genetic map of the proximal end of mouse chromosome 4 and the localization of the *inv* probe p3.2H. Probe 3.2H was mapped on mouse chromosome 4 by interspecific backcross analysis. (**A**) The segregation patterns of *inv* and flanking genes in 119 backcross animals that were typed for all loci. For individual pairs of loci, more than 119 animals were typed (*28*). Each column represents the chromosome identified in the backcross progeny that was inherited from the (C57BL/6J × *M. spretus*)F_1 parent. The shaded boxes represent the presence of a C57BL/6J allele. The number of offspring inheriting each type of chromosome is listed at the bottom of each column. (**B**) A partial chromosome 4 linkage map showing the location of *inv* in relation to linked genes. Recombination distances between loci in centimorgans are shown to the left of the chromosome, and the human chromosomal locations are shown to the right. References for the human map positions of loci mapped in this study can be obtained from the Genomic Data Base, a computerized database of human linkage information maintained by The William H. Welch Medical Library of the Johns Hopkins University (Baltimore, Maryland).

spretus–specific Bam HI restriction fragments (*15*, *16*) were used to follow the segregation of the *inv* locus. The mapping results indicated that *inv* is located in the proximal region of the mouse chromosome 4 and is linked to the *v-mos* oncogene homolog (*Mos*), the thyrotropin α subunit (*Tsha*), and the gene for hexabrachion (*Hxb*, also known as tenascin) loci (Fig. 3). Cytogenetic examination of the karyotype of the transgenic mice revealed no visible abnormalities of chromosome 4. Because *iv* has been mapped to chromosome 12 (*17*), the mapping of *inv* to chromosome 4 confirms that *inv* and *iv* are two separate genes.

One of the earliest manifestations of left-right asymmetry in mice is the pattern of embryonic turning (*18*). Murine embryos rotate from an initial lordotic orientation to a fetal position between E8.5 and E9.5 (Fig. 4). Embryonic rotation normally occurs in a clockwise fashion when viewed along the body axis from the cranial toward the caudal end (*19*). The right side of the embryo rotates over, and the left side rotates under the longitudinal axis. As a consequence of this rotation, the vitelline vessels become located along the left side of the body (Fig. 4B). Reversal of the direction of turning reverses the relation of the vitelline vessels relative to the body (Fig. 4B).

To examine whether *inv* mice exhibit an altered pattern of embryonic turning, we superovulated hemizygous transgenic females and mated them to hemizygous transgenic males to establish timed pregnancies; embryos were harvested after embryonic rotation was completed (Fig. 4A). Sixty embryos at E9.5 were examined and also assayed for homozygosity by Southern hybridizations with probe p3.2H. In hemizygous and nontransgenic embryos, the vitelline vessels were located on the left side of the body. In contrast, all 16 homozygous embryos had vitelline vessels situated on the right side of their bodies. This suggests that the direction of embryonic turning is reversed in all *inv/inv* embryos. Cardiac looping (the direction of bending of the embryonic heart tube) was examined in 29 embryos. All 21 nontransgenic and hemizygote embryos had a normal cardiac d-loop (*20*). Six out of 8 homozygous (*inv/inv*) embryos had an inverted cardiac l-loop, and the direction of looping was ambiguous in the other two.

Previous mutations and experimental manipulations have yielded an approximately 50% reversal of left-right asymmetry (*21*). Models for establishing handed asymmetry have been proposed (*5*, *18*, *21*, *22*) in which consistent reversal of asymmetry was suggested as possible but not very plausible (*5*, *18*). Our studies suggest that the direction of embryonic turning can become uniformly reversed in the absence of proper instruction from the *inv* gene. Developmentally, the direction of turning is tightly linked to the future orientation of the gut. However, the polarity of other organs such as heart and spleen does not always coincide with the direction of embryonic turning, which supports previous observations that organ primordia can acquire left-right axial information independently (*23*).

Because the *inv* mutation is recessive and caused by a transgenic integration event, it is likely to represent a loss-of-function mutation. This inference leads us to propose the existence of a default or alternative pathway for the determination of left-right asymmetry. In the absence of instruction from the *inv* gene, the default pathway consistently establishes an inverted left-right polarity. When *inv* is active, it overrides or reverses the default pathway, thereby initiating the establishment of the normal left-right polarity. Organ primordia appear to respond to the left-right asymmetry established by either the default or *inv* pathways. Although the default pathway is sufficient to produce 100% reversal of embryonic rotation and of stomach orienta-

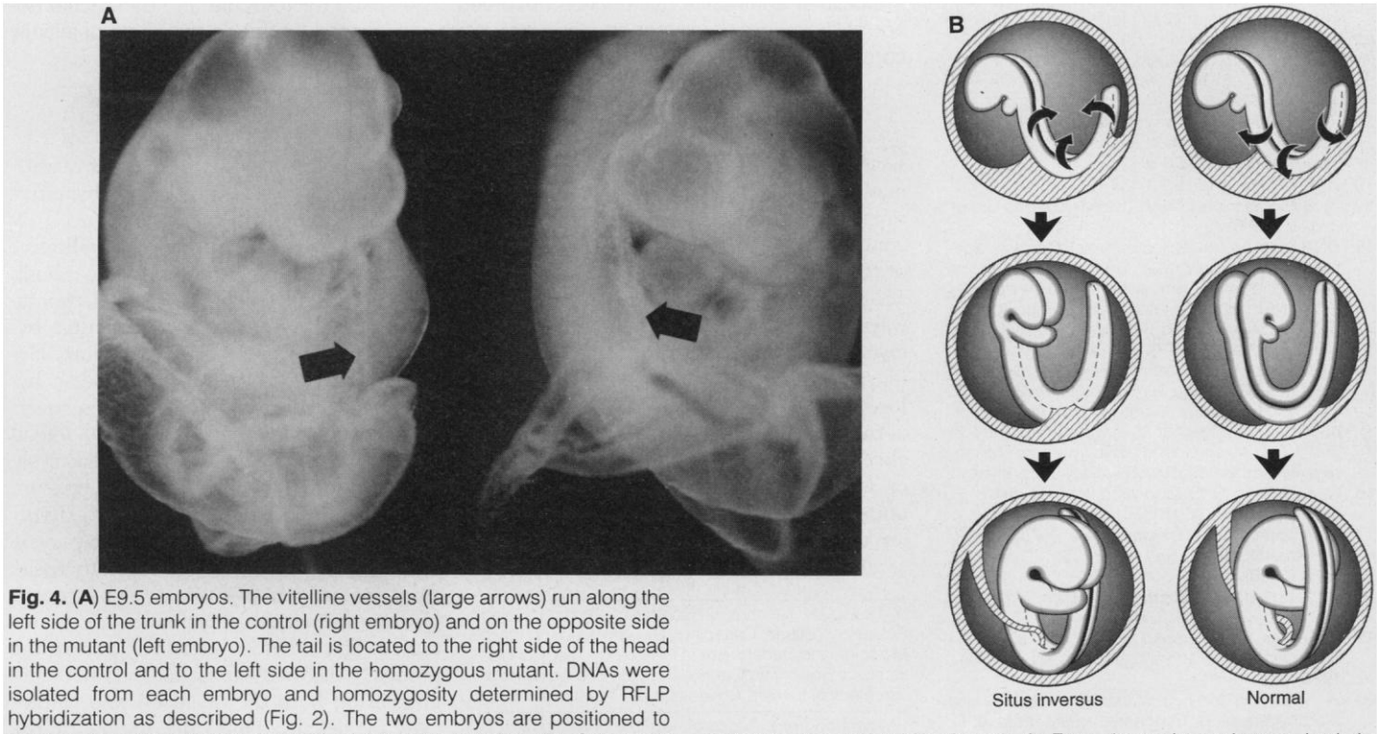

Fig. 4. (**A**) E9.5 embryos. The vitelline vessels (large arrows) run along the left side of the trunk in the control (right embryo) and on the opposite side in the mutant (left embryo). The tail is located to the right side of the head in the control and to the left side in the homozygous mutant. DNAs were isolated from each embryo and homozygosity determined by RFLP hybridization as described (Fig. 2). The two embryos are positioned to display the mirror-image reversal of left-right polarity. (**B**) Schematic topological representations of embryonic turning. Top: Lateral views of E8.5 embryos before turning. Middle: Embryonic rotation approximately two-thirds of the way to completion. Bottom: E9.5 embryos after turning. The midline of the dorsal side (the neural tube) is indicated by a thick solid line; the midline of the ventral side is indicated by a dotted line. The shaded area represents the yolk cavity, and the cross-hatched regions indicate extra-embryonic tissues. At E8.5, the embryos have a lordotic curvature and are depicted with the anterior to the left and the posterior to the right. The two alternative directions of embryonic turning are indicated by curved arrows (upper drawings). Notice that the vitelline vessels (indicated by the cross-hatched regions connected to each embryo at E9.5) become located on opposite sides of the embryos as a consequence of the opposite directions of turning.

tion, the pathway may not be sufficient to unambiguously specify polarity in other organs such as heart and spleen, resulting in heterotaxia. In any case, the *inv* mutation provides a new model system for studies on the specification of left-right polarity during vertebrate development.

REFERENCES AND NOTES

1. K. P. Hummel and D. B. Chapman, *J. Hered.* **50**, 10 (1959).
2. W. M. Layton, *ibid.* **67**, 336 (1976).
3. M. Kartagener and A. Horlacher, *Schweiz. Med. Wochenschr.* **65**, 782 (1935).
4. J. Torgeson, *Arch. Pathol.* **47**, 566 (1949).
5. M. J. Morgan, in *Biological Asymmetry and Handedness*, G. R. Bock and J. Marsh, Eds. (Wiley, Chichester, United Kingdom, 1991), pp. 234–250.
6. T. Yokoyama *et al.*, *Nucleic Acids Res.* **18**, 7293 (1990).
7. T. Yokoyama and P. A. Overbeek, unpublished results.
8. B. A. Afzelius, *Science* **193**, 317 (1976).
9. W. Brinkley, personal communication.
10. Large molecular weight DNA was isolated from 3-day-old mutant mouse kidney as described (*11*). The DNA was digested partially with Sau 3AI; fragments larger than 15 kb were isolated by fractionation on a sucrose gradient (*12*) then ligated to the Lambda EMBL3 vector (Stratagene) that had been digested with Bam HI. Ligation products were packaged in vitro with Gigapack II (Stratagene). Approximately 5×10^5 plaques were screened with the tyrosinase minigene TyBS (*6*) as a probe. Positive plaques were purified through three rounds of screening then assayed for the presence of tyrosinase cDNA sequences with the use of the polymerase chain reaction (*6*). Genomic sequences from the λ clones were subcloned and tested for single-copy sequences by Southern hybridization (*13*).
11. J. L. Longmire, K. L. Albright, A. K. Lewis, L. J. Meincke, C. E. Hildebrand, *Nucleic Acids Res.* **15**, 859 (1987).
12. J. H. Weis, in *Current Protocols in Molecular Biology*, F. M. Ausubel *et al.*, Eds. (Wiley, New York, 1987), 5.3.2–5.3.8.
13. R. F. Seldon, *ibid.*, 2.9.1–2.9.10.
14. N. G. Copeland and N. A. Jenkins, *Trends Genet.* **7**, 113 (1991).
15. DNA isolation, restriction enzyme digestion, agarose gel electrophoresis, Southern blot transfer, and hybridization were performed essentially as described (*16*). The *inv* genomic probe (p3.2H) (Fig. 2A) was labeled with [α-^{32}P]deoxycytidine 5′-triphosphate (dCTP) with a nick translation labeling kit (Boehringer Mannheim). A 9.6-kb fragment was detected in Bam HI–digested C57BL/6J DNA and 6.6- and 3.7-kb fragments were detected in Bam HI–digested *M. spretus* DNA. The 6.6- and 3.7-kb *M. spretus*–specific fragments cosegregated and were followed in backcross mice.
16. N. A. Jenkins, N. G. Copeland, B. A. Taylor, B. K. Lee, *J. Virol.* **43**, 26 (1982).
17. M. Brueckner, L. A. D'Hoostelaere, A. Calabro, P. D'Eustachio, *Proc. Natl. Acad. Sci. U.S.A.* **86**, 5035 (1989).
18. N. A. Brown, A. McCarthy, L. Wolpert, in (*5*), pp. 182–201.
19. K. Theiler, in *The House Mouse: Atlas of Embryonic Development* (Springer-Verlag, New York, 1989), pp. 40–42.
20. W. M. Layton and F. J. Manasek, in *Etiology and Morphogenesis of Congenital Heart Disease*, R. Van Praugh and A. Takao, Eds. (Futura, Mount Kisco, NY, 1980), pp. 109–128.
21. N. A. Brown and L. Wolpert, *Development* **109**, 1 (1990).
22. M. J. Morgan and M. C. Corballis, *Behav. Brain Sci.* **2**, 270 (1978).
23. H. J. Yost, *Nature* **357**, 158 (1992).
24. J. D. Ceci, L. D. Siracusa, N. A. Jenkins, N. G. Copeland, *Genomics* **5**, 699 (1989).
25. C.-L. Hsieh, U. Dorries, M. Schachner, U. Franke, *Mammalian Genome* **1**, S522 (1991).
26. E. L. Green, *Genetics and Probability in Animal Breeding Experiments*, (Oxford Univ. Press, New York, 1981), pp. 77–113.
27. A. P. Feinberg and B. A. Vogelstein, *Anal. Biochem.* **137**, 266 (1984).
28. The ratios of the total number of mice that exhibited recombinant chromosomes to the total number of mice analyzed for each pair of loci and the most likely gene order are: centromere-*Mos* (9/122) *Tsha* (7/121) *inv* (19/190) *Hxb*. The recombination frequencies (expressed as genetic distances in centimorgans ± SE) are: *Mos* (7.4 ± 2.4) *Tsha* (5.8 ± 2.1) *inv* (10.0 ± 2.2) *Hxb*. Descriptions of the probes and restriction fragment length polymorphisms for the loci linked to the *inv* locus, including *Mos* and *Tsha*, have been reported previously (*24*). One locus used to position *inv* on chromosome 4 has not been reported previously for our interspecific map. The probe for the *Hxb* locus was a 2-kb mouse cDNA from the 3′ end of the gene (*25*) that detected 7.0-, 6.4-, 5.8-, 1.2-, and 1.0-kb fragments in Pvu II–digested C57BL/6J DNA and 9.0-, 6.4-, 5.6-, 1.4-, 1.2-, and 1.0-kb fragments in Pvu II–digested *M. spretus* DNA. The 9.0-kb *M. spretus*–specific fragment was followed in this analysis. Recombination distances were calculated as described (*26*) with the computer program SPRETUS MADNESS (unpublished program). We determined the gene order by minimizing the number of recombination events required to explain the allele distribution patterns.

29. We wish to thank R. Collins for providing the SI/Col mice, W. Brinkley and D. Turner of the Cell Biology Microscopy Core Laboratory for electron microscopy, R. Geske for help with photography and histology, L. Kairewich for artistic assistance, D. J. Gilbert for excellent technical assistance, T. Reid for help with the manuscript, and G. MacGregor for critical reading of the manuscript. This research was supported, in part, by NIH grant HD25340 (P.A.O.) and by the National Cancer Institute, Department of Health and Human Services, under contract NO1-CO-74101 with ABL. All mice used in this study were handled in accordance with the NIH Guide for the Care and Use of Laboratory Animals with protocols approved by the Animal Protocol Review Committee of the Baylor College of Medicine.

1 December 1992; accepted 22 March 1993

Cytoskeletal Role in the Contractile Dysfunction of Hypertrophied Myocardium

Hiroyuki Tsutsui,* Kazuaki Ishihara,† George Cooper IV‡

Cardiac hypertrophy in response to systolic pressure loading frequently results in contractile dysfunction of unknown cause. In the present study, pressure loading increased the microtubule component of the cardiac muscle cell cytoskeleton, which was responsible for the cellular contractile dysfunction observed. The linked microtubule and contractile abnormalities were persistent and thus may have significance for the deterioration of initially compensatory cardiac hypertrophy into congestive heart failure.

Cardiac hypertrophy is the response to many physiological and pathological deviations from normal homeostasis that have in common increased hemodynamic loading of the heart (*1*). This growth process proceeds until the load stimulus is abated by way of a renormalization of stress per unit of myocardial mass. Hypertrophy fails to be functionally compensatory when either the load increase exceeds the growth capacity of the terminally differentiated cardiac muscle cell (or cardiocyte) to renormalize stress or when the contractile performance per unit mass of hypertrophied myocardium is less than that of normal myocardium. Thus, cardiac compensation for an increased load may be imperfect because of either quantitative or qualitative defects of hypertrophied myocardium.

This study investigated the qualitative defects of hypertrophied myocardium, which may underlie the frequent deterioration of initially compensatory cardiac hypertrophy into congestive heart failure. Hemodynamic overloads causing cardiac hypertrophy consist of either (i) volume overloading, in which an increased blood volume is pumped during each cardiac cycle against a normal impedance, or (ii) pressure overloading, in which a normal blood volume is pumped during each cardiac cycle against an increased impedance. In tissue from the volume-overloaded right ventricle, normal cardiac mechanics are maintained (*2*), whereas pressure overloading produces distinctly abnormal cardiac mechanics on both the tissue (*3*) and cardiocyte (*4*) levels. Thus, the nature of the stress rather than hypertrophy itself causes the qualitative defects of myocardium hypertrophying in response to a pressure overload, and the contractile defect lies in the cardiocyte.

Although potential causes for the abnor-

H. Tsutsui, K. Ishihara, G. Cooper IV, Gazes Cardiac Research Institute, Cardiology Division, Department of Medicine and Department of Physiology, Medical University of South Carolina and the Veterans Administration Medical Center, Charleston, SC 29401.

*Present address: Research Institute of Angiocardiology and Cardiovascular Clinic, Kyushu University School of Medicine, 3-1-1 Maidashi, Higashi-ku, Fukuoka, 812, Japan.

†Present address: Department of Pediatric Cardiovascular Surgery, Heart Institute of Japan, Tokyo Women's Medical College, 8-1 Kawada-cho, Shinjuku-ku, Tokyo, 162, Japan.

‡To whom correspondence should be addressed.